

IMPEDANCE AND INSTABILITY STUDIES IN LEIR WITH XENON

N. Biancacci, H. Bartosik, M. Gasior, S. Hirlander,
A. Latina, T. Levens, E. Métral, CERN, Geneva, Switzerland,
M. Migliorati, University of Rome “La Sapienza” and INFN-Roma I

Abstract

In 2017, the LEIR accelerator has been operated with Xe^{39+} beam for fixed target experiments in the SPS North Area. The different ion species, with respect to the standard Pb^{54+} , allowed for additional comparative measurements of tune shift versus intensity at injection energy both in coasting and bunched beams. The fast transverse instability observed for high accumulated intensities has been as well characterized and additional observations relevant to impedance have been collected from longitudinal Schottky signal and BTF measurements. The results of these measurements are summarised and compared to the currently developed machine impedance model.

INTRODUCTION

The LEIR machine accelerates ions from 4.2 MeV/n kinetic injection energy to 72.2 MeV/n at extraction to the PS. During 2017, a special run was planned: in place of Pb^{54+} ions, Xe^{39+} ions were accelerated for fixed target experiments in the SPS and for collisions in the LHC: both low and high intensity cycles (so called EARLY and NOMINAL cycles) were setup in order to deliver the required beam intensity at extraction. The change of particle specie, allowed to compare and complement the present impedance and coherent instability model, so far developed and benchmarked during the Pb^{54+} runs [1]. This work is structured as follows: the first section will cover the longitudinal impedance measurements performed by means of Schottky peaks separation as a function of the intensity; the second section will show the results of the transverse impedance measurements by means of tune shift versus intensity; the last section is devoted to the transverse coherent instability observations and to the BTF complementary measurements.

LONGITUDINAL IMPEDANCE MEASUREMENTS

The reactive part of the longitudinal impedance can be inferred, in strongly cooled coasting beams, from shift of the longitudinal coherent beam modes versus intensity [2]. These modes can be observed with a Schottky system [3] and would appear as in Fig. 1, where the LEIR intensity accumulation and phase space cooling process is depicted: the more the intensity is accumulated, the more the Schottky power density spectrum peaks around the slow and fast longitudinal wave frequencies.

The coherent longitudinal frequency mode shift with intensity at the n^{th} harmonic of a coasting beam is given by [4]

$$\Delta f = n f_0 \sqrt{j \frac{Z_l}{n} |\eta| \frac{Z/A e I}{p_0 \beta c 2\pi}} \quad (1)$$

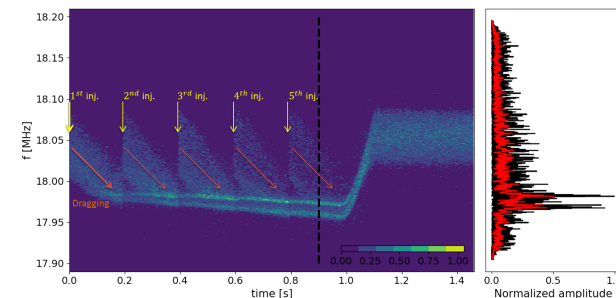


Figure 1: Left: Schottky power density spectrum during accumulation and cooling process in LEIR: injection and cooler energy dragging processes are highlighted. Right: spectrum at 900 ms with (red) and without (black) moving window averaging for noise reduction.

with f_0 the revolution frequency, Z_l the machine longitudinal beam coupling impedance, η the slip factor, Z/A the charge over mass ratio, β relativistic velocity factor, c the speed of light, p_0 momentum per nucleon, e elementary charge, $I = e f_0 N$ circulating beam current for N number of circulating charges.

Figure 2 shows the comparison between measurement and theoretical expectation from indirect space charge only (ISC) computed with the current LEIR longitudinal impedance model, and from direct and indirect space charge (ISC+DSC) computed with an approximate model accounting for the beam of circular cross section of radius $a = 2$ mm in a circular beam pipe of 2.7 cm (LEIR average aperture half gap) [5]. As expected, the agreement is satisfactory only when the direct space charge contribution is accounted for. The remaining discrepancy suggests that the indirect space charge impedance model could be $\approx 20\%$ higher than expected from the impedance model. The discrepancy above $N = 3 \cdot 10^{10}$ charges can be justified by the relative increase of emittance for high intensity as measured at the beam gas ionization monitor.

TRANSVERSE IMPEDANCE MEASUREMENTS

The reactive part of the transverse impedance can be inferred probing the tune variation versus intensity. In addition to the already performed measurements in coasting and bunched beams [1], we performed tune shift measurements in coasting beam with the Xe beam. The change in

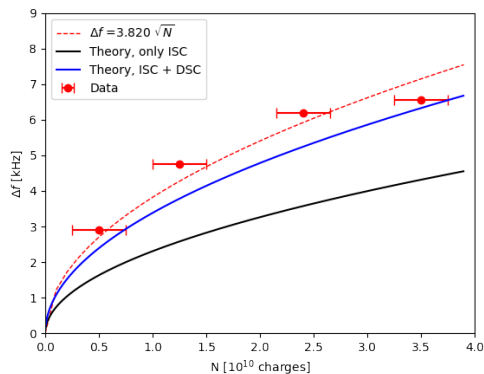


Figure 2: Peak split versus intensity measured from Schottky spectrum and computed with Eq. (1) without (black) and with (blue) longitudinal direct space charge (DSC).

charge over mass ratio is expected to increase the tune shift by $\approx 20\%$. Figure 3 shows the comparison between the measured and predicted tune shift for *Pb* and *Xe* as measured between 2016 and 2017. The *Xe* measurements have been scaled to the charge over mass ratio of *Pb* and are in good agreement within the large tune spread. On average, the model is explaining the 80% of the machine total reactive impedance.

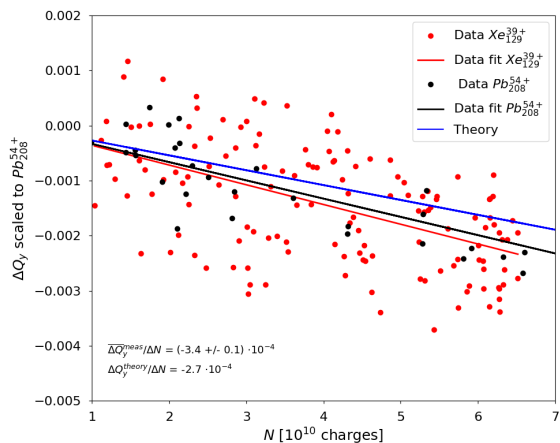


Figure 3: Tune shift versus intensity in coasting beam for both *Xe* and *Pb* ions, compared with prediction: 80% of the impedance model is explained.

INSTABILITY OBSERVATIONS AND BTF

The LEIR machine needs to be operated with transverse feedback active for the full cycle. This is done in order to fight a fast coherent vertical instability observed at 1.9 MHz with a rise time of $25 \text{ ms}/10^{10}$ charges corresponding to an equivalent resonator impedance centered on the transverse coherent line number $n = -8$ with shunt impedance $R_{sh} = 28 \text{ M}\Omega/\text{m}$ [1].

During the 2017 run, it was possible to perform further tests in order to characterize the instability. Figure 4 shows

the instability growth rate for different Q' values once the transverse damper is switched off: we notice that the instability starts together/after the 100 kHz line which corresponds to the lowest frequency mode $n = -3$ driven by resistive wall impedance. For $Q' < 0$ only the $n = -3$ line is observed and the $n = -8$ seems to be stabilized. The instability is observed with a rise time of 20 ms at $N = 5.3 \cdot 10^{10}$ charges, i.e. corresponding to a growth rate of $10 \text{ s}^{-1}/10^{10}$ charges which is 4 times lower than the corresponding one measured with *Pb*. The discrepancy could be due to differences in the working point which can affect the overlap of the unstable line with the equivalent resonator impedance. It is interesting to notice that also the $n = -3$ line exhibits a comparable growth rate, far from the expected $0.3 \text{ s}^{-1}/10^{10}$ charges predicted by the impedance model. This behaviour was present, but less evident, also during the studies with *Pb* and will be subject of further investigations during the 2018 run.

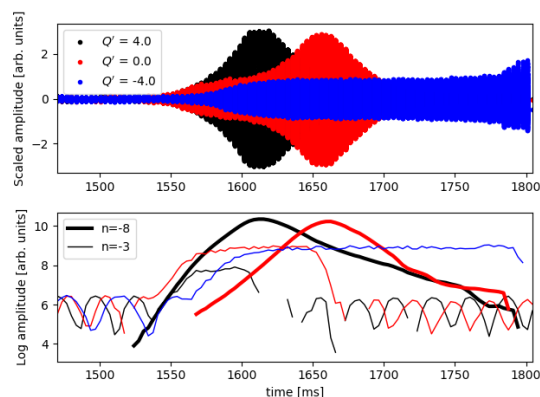


Figure 4: Instability evolution varying Q' . Measurement performed with a coasting beam of $N = 5.3 \cdot 10^{10}$ charges, without damper and after cooling process.

In order to better understand the source of the instability, transverse beam transfer function (BTF) measurements were performed. The BTF technique is well established (see for example [6, 7]) and consists in recording the dipole motion response B of the beam at a pickup, once a sinusoidal excitation A at frequency ω_d is applied from a kicker. The transverse BTF is defined as

$$BTF = 2\omega_\beta \Delta\omega \frac{B}{A} = \frac{1}{\mathcal{D}(u) + \xi/\Delta\omega} \quad (2)$$

with ω_β betatron angular frequency, $\Delta\omega$ betatron frequency spread, ξ the transverse complex mode frequency shift [4] proportional to the intensity and the transverse impedance sampled at the driven frequency ω_d , $\mathcal{D}(u)$ the stability diagram [8] with $u = (\omega_\beta + n\omega_0 - \omega_d)/\Delta\omega$, and ω_0 the revolution frequency. Measuring the BTF at different intensities, it is possible to access information both on the stability diagram shape and the transverse impedance.

In LEIR, an Agilent Vector Network Analyzer (VNA) E5071C was connected to the transverse damper kicker and

Content from this work may be used under the terms of the CC BY 3.0 licence (© 2018). Any distribution of this work must maintain attribution to the author(s), title of the work, publisher, and DOI.

the response was recorded from the base band tune meter (BBQ) pickup [9] and sent back to the VNA. Figures 5 and 6 show the beam response and BTF reconstruction around the $n = -3$ and $n = -8$ unstable lines for $Q' = 0$, with active damper and after the cooling process. Due to the finite signal time of flight and the large noise, corrections on the BTF phase signal have been performed both with time gating [10] and averaging. The BTF response presents a double peak structure which can be attributed to the previous cooling process: this is responsible for the circle-like shape at the center of the stability diagram as also predicted in [11]. A clear shift is present, mainly in the imaginary axis direction, i.e. due to the real part of the transverse impedance. Also, an enlargement of the stability diagram due to the larger momentum spread due to the longer accumulation phase is visible. The magnitude of the BTF can be considered only qualitatively for the moment, due to the presence of attenuators and filters (before damper excitation and in the BBQ front-end) that will need to be characterized and included for future measurements. A qualitative trend of the growth rate $\tau^{-1} = \text{Im}(\xi)$ versus frequency (i.e. corresponding to the real part of the vertical impedance) is shown in Fig. 7 where the vertical displacements of the stability diagram have been recorded as a function of frequency and normalized in order to match the growth rate shown in Fig. 4: both lines $n = -3$ and $n = -8$ exhibit similar growth rates, and a broadband impedance increase can be appreciated above 500 kHz, the source of which will be subject of further investigation.

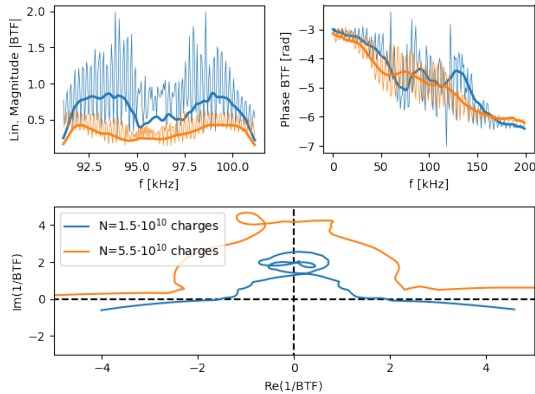


Figure 5: BTF response around $n = -3$ in magnitude (top-left) and phase (top-right) with and without gating and averaging corrections. The stability diagram (bottom) refers to $Q' \approx 0$ at different intensities, with damper after cooling.

CONCLUSIONS

The LEIR machine was operated with Xe^{39+} during 2017. The change of particle type with respect to the standard Pb^{54+} offered the possibility to perform comparative and additional impedance and instability studies.

The longitudinal reactive impedance of the machine was characterized by means of tracking the longitudinal coherent mode split versus intensity on the Schottky signal. The

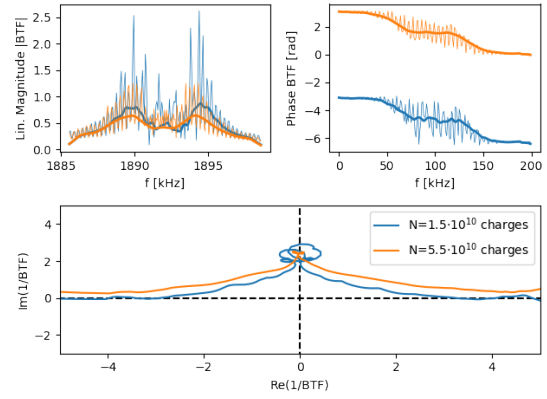


Figure 6: Same as previous figure but for $n = -8$.

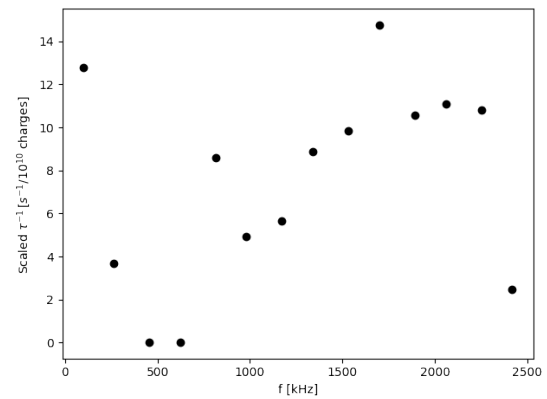


Figure 7: Growth rate τ^{-1} deduced from shift of the stability diagram for different beam frequencies. The magnitude is scaled to match the $n = -8$ growth rate in Fig. 4.

vertical reactive impedance was characterized by measuring the tune shift versus intensity in coasting beam regime. The agreement achieved with respect to theory is acceptable and in agreement with the impedance model within 80%.

The strong vertical instability recorded with Pb^{54+} was also observed with Xe^{39+} . A detailed analysis of the instability growth process showed that the unstable modes $n = -3$ and $n = -8$ are growing together at least at the beginning of the instability process. Both modes exhibit higher growth rates with respect to the present impedance model. Stabilization occurred for $Q' = -4$ on mode $n = -8$.

BTF measurements were performed and confirmed qualitatively the large impedance increase at both unstable lines as well as a broadband increase above 500 kHz, the origin of which, will be subject for future refinement of the impedance and instability model.

The authors would like to thank the SPS-LEIR operation team for the support during the beam measurements as well as R. Scrivens and R. Alemany Fernandez.

REFERENCES

- [1] N. Biancacci, E. Métral, M. Migliorati, and T. L. Rijoff. LEIR impedance model and coherent beam instability observations. In *8th International Particle Accelerator Conference*, pages 3159–3162, paper WEPIK094, Copenhagen, Denmark, 14–19 May 2017.
- [2] H. Poth. Electron Cooling: Theory, Experiment, Application. *Phys. Rep.*, 196 (CERN-EP 90-04):135 – 297, 1990.
- [3] S. Cocher and I. Hofmann. On The Stability And Diagnostics Of Heavy Ions In Storage rings With High phase Space Density. *Part. Accel.*, 34 (GSI-89-61):189–210, Aug 1989.
- [4] J. L. Laclare. Introduction to coherent instabilities: coasting beam case. *CAS - CERN Accelerator School, Gif-sur-Yvette, France*, 1984.
- [5] R. L. Gluckstern. Analytic methods for calculating coupling impedances. (CERN-2000-011), 2000.
- [6] A. W. Chao. *Physics of Collective Beam Instabilities in High Energy Accelerators*. John Wiley & Sons, Inc., New York, 1993.
- [7] S. Paret. *Transverse Schottky spectra and beam transfer functions of coasting ion beams with space charge*. PhD thesis, Technische Universität, Darmstadt, April 2010.
- [8] K. Hübner, A. G. Ruggiero, and V. G. Vaccaro. Stability of the coherent transverse motion of a coasting beam for realistic distribution functions and any given coupling with its environment. (CERN-ISR-TH-RF-69-23):7 p, Jul 1969.
- [9] M. Gasior and R. Jones. The principle and first results of betatron tune measurement by direct diode detection. (CERN-LHC-PROJECT-REPORT-853), CERN, Geneva, Switzerland, 2005.
- [10] F. Caspers, M. Chanel, and U. Oeftiger. A novel method of noise suppression in beam transfer function measurements. (CERN-PS-93-19-AR), CERN, Geneva, Switzerland, 1993.
- [11] K. Hübner and V. G. Vaccaro. Dispersion relations and stability of coasting particle beams. (CERN-ISR-TH-70-44), CERN, Geneva, Switzerland, 1970.